A Self-Powered Implantable Drug-Delivery System Using Biokinetic Energy

Peiyi Song, Shuangyang Kuang, Nishtha Panwar, Guang Yang, Danny Jian Hang Tng, Swee Chuan Tjin, Wun Jern Ng, Maszenan Bin Abdul Majid, Guang Zhu, Ken-Tye Yong,* and Zhong Lin Wang**

With the rapid growth of microscale implantable devices, their applications in diagnostic sensing,[1] stimulating tissues/organs,[2,3] monitoring body functions,[4,5] imaging,[6] and delivering drugs[7,8] have been demonstrated. For example, implantable drug-delivery system (iDDS) has made localized treatment feasible with high drug delivery efficiency and great controllability in delivery time and rate.[7,9,10] Such devices are useful in the treatment of diabetes, ocular disease, and cancer. So far, most of these devices need an external power source such as lithium-ion batteries for activation. Desirably, iDDS is greatly miniaturized, and the battery is smaller. However, it has a limited lifetime due to the limited energy storing capacity of the small size battery. This calls for frequent unwanted surgeries for device replacement for a sustainable treatment. Apart from the risk and cost involved in using iDDS, the frequent need for surgeries also reduces patient's willingness of adapting these new therapies. To overcome this challenge of continuously powering an iDDS, it is critical to find a sustainable powering solution. On one hand, wireless power transmission is being studied.[5,11] Researchers have demonstrated the use of metal coil in the device to harvest energy from radio-frequency signal generated from a transmitter for powering a drug-delivery pump.[12] But in this method, a complicated external signal generator/transmitter is needed and the working conditions for remote power transmission are strict. On the other hand, implantable materials that harvest energy from chemical, mechanical, electrical, and thermal processes in the human body have been demonstrated, such as using biochemical reaction,[13] the electric potentials in human body,[14] mechanical movements of body parts,[15] and the vibration of organs using piezoelectric nanogenerator.[16] However, none of these solutions are applied in implantable drug-delivery applications due to their relatively large footprint and small output.

Recently, researchers have invented the triboelectric nanogenerator (TENG).[17,19] TENG offers an effective method to harvest ambient mechanical energy and transfer it into electricity. Its working principle is based on the combination of contact electrification and electrostatic induction.[20] When two tribomaterials with opposite polarity come in contact—separate with each other, an electrification potential is built between the two tribomaterials. The potential difference leads contact-induced charges to transfer between the electrodes which are attached on the tribomaterials. The current could be used for powering devices.[21,22] TENG has a simple structure, thus it can be greatly miniaturized and fabricated using soft materials.[19] At the same time, TENG generates a strong output that ranges up to a few milliwatts (mW).[23] Therefore, TENG can be implanted to harvest the energy from body/organ's motion and engineered as an ideal power source for implantable biomedical devices. For example, Zheng et al. have demonstrated the use of an implanted TENG to power a pacemaker in vivo. The study validated the feasibility for developing TENG-based implantable biomedical devices.[2] The sustained biokinetic energy would make implantable devices self-powered with the help of TENG. Such TENG-enabled implantable devices would be a promising approach toward self-powered iDDS with sustained biokinetic energy.

In this communication, we present the first TENG-based self-powered iDDS for drug-delivery applications. The device comprises an electrochemical microfluidic pump which is powered by TENG. The working performance of the self-powered device is characterized. As a demonstration, trans-sclera drug delivery is performed in porcine eyes ex vivo. The iDDS derives its functional power from the energy harvested from human body's motion through TENG for drug delivery.

Fabrication Result: The self-powered iDDS is composed of an energy harvesting system (TENG) and a drug pumping system (iDDS). **Figure 1**B illustrates the schematic diagram

Dr. P. Song, Prof. S. C. Tjin, Prof. W. J. Ng,
Dr. M. B. A. Majid, Prof. K.-T. Yong
Nanyang Environment and Water Research Institute
Nanyang Technological University
1 Cleantech Loop, CleanTech One #06-08
Singapore 637141, Singapore
E-mail: ktyong@ntu.edu.sg
Dr. P. Song, N. Panwar, G. Yang,
Prof. S. C. Tjin, Prof. K.-T. Yong
School of Electrical and Electronic Engineering
Nanyang Technological University
50 Nanyang Avenue, Singapore 639798, Singapore
S. Kuang, Prof. G. Zhu, Prof. Z. L. Wang
Beijing Institute of Nanoenergy and Nanosystems
Chinese Academy of Sciences
Beijing 100083, China
E-mail: zhuguang@binn.cas.cn; zlwang@gatech.edu
D. J. H. Tng
Duke-NUS Medical School
8 College Road, Singapore 169857, Singapore
Prof. Z. L. Wang
School of Material Science and Engineering
Georgia Institute of Technology
Atlanta, GA 30332-0245, USA

DOI: 10.1002/adma.201605668

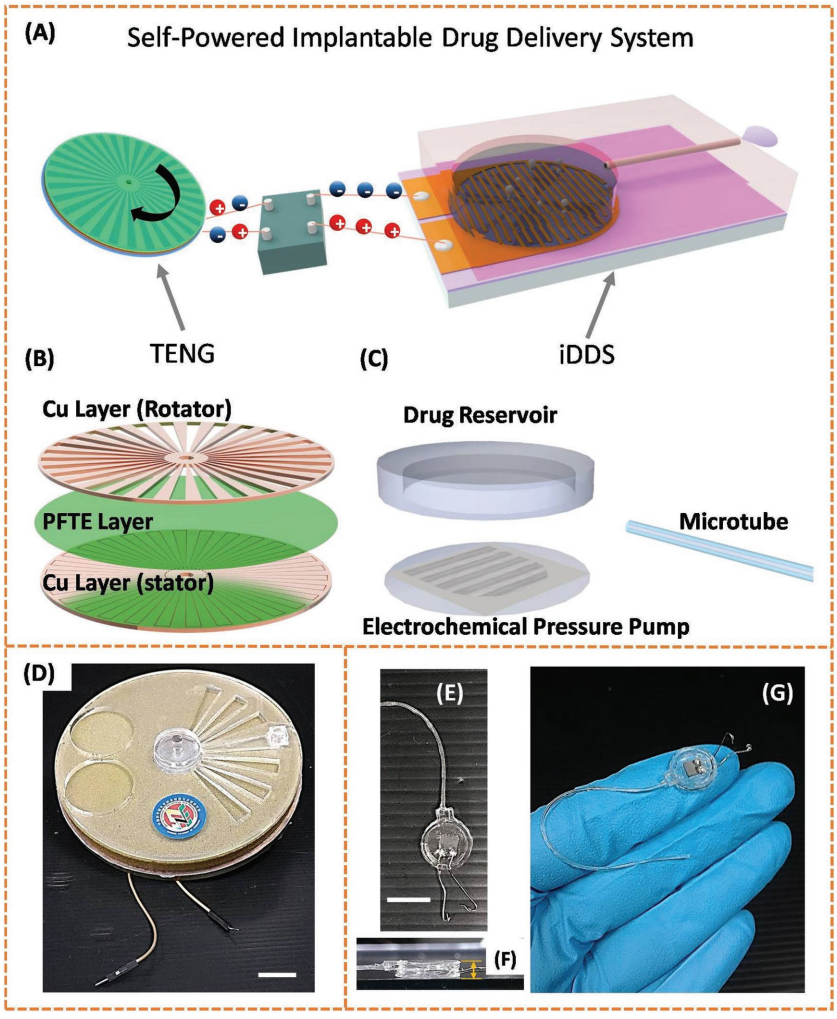

Figure 1. Structural designs and photographs of the TENG and the iDDS. A) Schematic illustration of the TENG-based iDDS. B) Schematic illustration of the parts in TENG. C) Schematic illustration of the parts in iDDS. D) Photograph of the TENG packaged in glass epoxy. The scale bar indicates 10 mm. E) Photograph of the iDDS. The scale bar indicates 10 mm. F) Side-view photograph of the iDDS. The thickness measured is 2 mm. G) Photograph of the iDDS on a human hand.

of the TENG. Two layers of metal Cu patterned with radial-arrayed strips were assembled as a rotator and a stator. A layer of poly(tetrafluoroethylene) (PTFE) film was pasted in between the two metal layers as the electrification material. This simple structure makes TENG easily miniaturized and flexible. The photograph of the TENG packaged in glass epoxy is presented in Figure 1D. Figure 1C illustrates the schematic diagram of the drug pumping system which comprises: i) the PDMS drug reservoir, ii) the PDMS microtube, and iii) a pair of Au electrodes on silicon substrate for electrochemical pumping, respectively. The dimension of the reservoir was determined to be 10 mm long, 10 mm wide, and 2 mm thick, which is suitable for subcutaneous implantation.[7] PDMS was used as the main material for constructing the iDDS for its proven highly biocompatibility in implantation.[7] Another attractive feature of using a PDMS drug reservoir is its refillability for its drug contents.[11] The proposed TENG-based iDDS can be suitably implanted in subcutaneous tissues or under the eye's sclera, which are easily accessed by a syringe. Also the silicone-based drug reservoir enables multiple needle pokes without causing any leakages. The PDMS microtube connected to the reservoir had a length of up to 100 mm and an outer diameter of 0.5 mm and inner diameter of 0.3 mm. The PDMS microtube takes advantage of small size and great elasticity thus it can be easily implanted to target sites by a minimally invasive implantation surgery. The use of this microtube alleviates the need to implant the entire device deeply into the tissue. Au electrodes, 5 mm long, 5 mm wide, and 0.5 mm thick, were constructed on a silicon substrate through photolithography to achieve 40 µm pattern sizes. The substrate was integrated at the base of the PDMS drug reservoir. The photograph of the proposed iDDS is presented in Figure 1E–G.

Self-Powered Drug Pumping with a TENG: To achieve self-powered drug pumping, the TENG-based energy-harvesting system and the drug pumping system were connected using wires. **Figure 2** shows the working principle of this application. The basic working mechanism of TENG was reported previously.[23] Briefly, upon rotation of TENG, the Cu grating on the rotator slides along the PTFE film, injecting electrons from rotator Cu to the PTFE film due to the contact electrification to build potential difference between the two materials. Thus, an AC current can be generated between the Cu electrodes on the stator. The whole process is demonstrated in Figure 2A. The open-circuit voltage and short-circuit current of TENG were measured and shown in **Figure 3**A,B. In our application, the output of the TENG was transformed and rectified to DC current before it was applied onto the Au electrodes for the electrochemical pressure pumping (Figure 3C,D). This ensured a continuous flow of electrons to the cathode, making it negatively charged and the anode electrode positively charged. The potential built between the Au electrodes initiated the water splitting process. According to the electrolysis effect, the water splitting process can be explained by the following Equation (1a) and (1b)

$$4OH^- \rightarrow 2H_2O + O_2 + 4e^- \,(\text{anode}) \tag{1a}$$

$$4H^+ + 4e^- \rightarrow 2H_2 \,(\text{cathode}) \tag{1b}$$

Oxygen and hydrogen gases were generated on the anode and cathode, respectively, to pressurize the drug reservoir (Figure 2B–E and **Figure 4**C,D). Eventually, the drug contents in the reservoir were pumped out through the microtube.

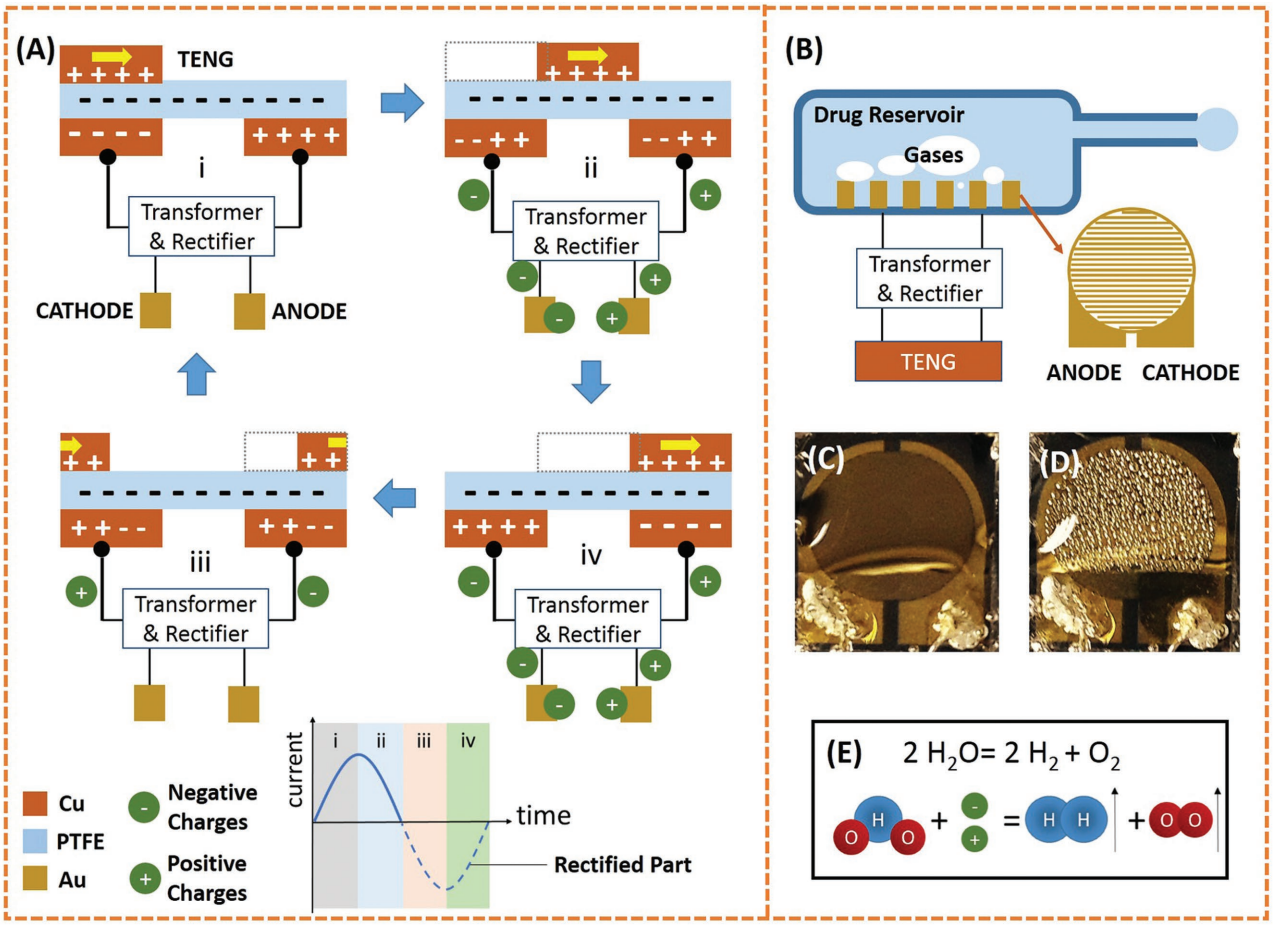

Figure 2. Working principle of the TENG-based self-powered iDDS. A) Schematic illustration of working principle of the TENG. B) Schematic illustration of the working principle of the electrochemical pressure pumping. C) Amplified photograph of the gold electrodes. D) Amplified photograph of the gold electrodes with air bubbles that were generated from electrochemical pressure pumping. E) Principle of water electrolysis.

The drug-delivery speed corresponds to the gas production rate in electrolysis, which is determined by the rate of generation of electrons in TENG, represented in terms of output current. It should however be noted that a small amount of drug ions could participate with the electrochemical reaction that may produce byproducts. To prevent this, a parylene-C membrane may possibly be placed on top of the electrochemical actuator to separate electrolytes (deionized (DI) water) and drug solutions in our next prototype (see Figure S4 in the Supporting Information). Parylene-C can also be coated on the poly(dimethylsiloxane) (PDMS) reservoir which could act as a sealing, anticorrosion, hydrophobic antifriction, and biocompatible barrier for iDDS.[24] PTFE deposition on the inner wall of drug reservoir is suggested to enhance its chemical compatibility.[25]

To increase the drug-delivery efficiency, we engineered the electrochemical pressure pump to enhance the output current of the TENG for a higher water splitting speed. In our electrochemical pressure pump, ultrapure DI water was used as the electrolyte. However, the large resistivity of ultrapure DI water (18.2 MΩ cm) makes TENG less efficient in electrolysis due to the small output current. Based on the definition of resistivity, the resistance in the electrolysis process can be defined as:

$$\text{Resistance}(\Omega) = \rho \frac{l}{A} \tag{2}$$

where ρ represents the electrical resistivity coefficient of pure water, l is the distance between the electrodes, and A is the cross-section area of the electrodes. To reduce the large resistance, we utilized an interdigital electrode design with a 40 µm gap between anode and cathode, which is much smaller than conventional electrode design (see the comparison in Figure 4A,B). Also, the cross-section areas in the interdigital electrode are increased by the fold of $2N - 1$ (N is the number of electrode's fingers) compared to conventional two finger electrodes. Thus, our design significantly reduced the resistance between the electrodes to about 10 kΩ. With this setting, the output current of TENG reached about 1.5 mA at an output voltage of 15 V (Figure 3C,D) under the rotating speed of 500 rpm, which is sufficient for electrochemical pumping (Figure 4C–F). However, it is important to note that, the drug content used in pumping would result in a different resistivity than that with ultrapure DI water. To achieve a large output current from TENG, the gap distance between the electrodes should be modified to achieve the loading resistance matching with TENG. For another solution, a two-chamber drug reservoir

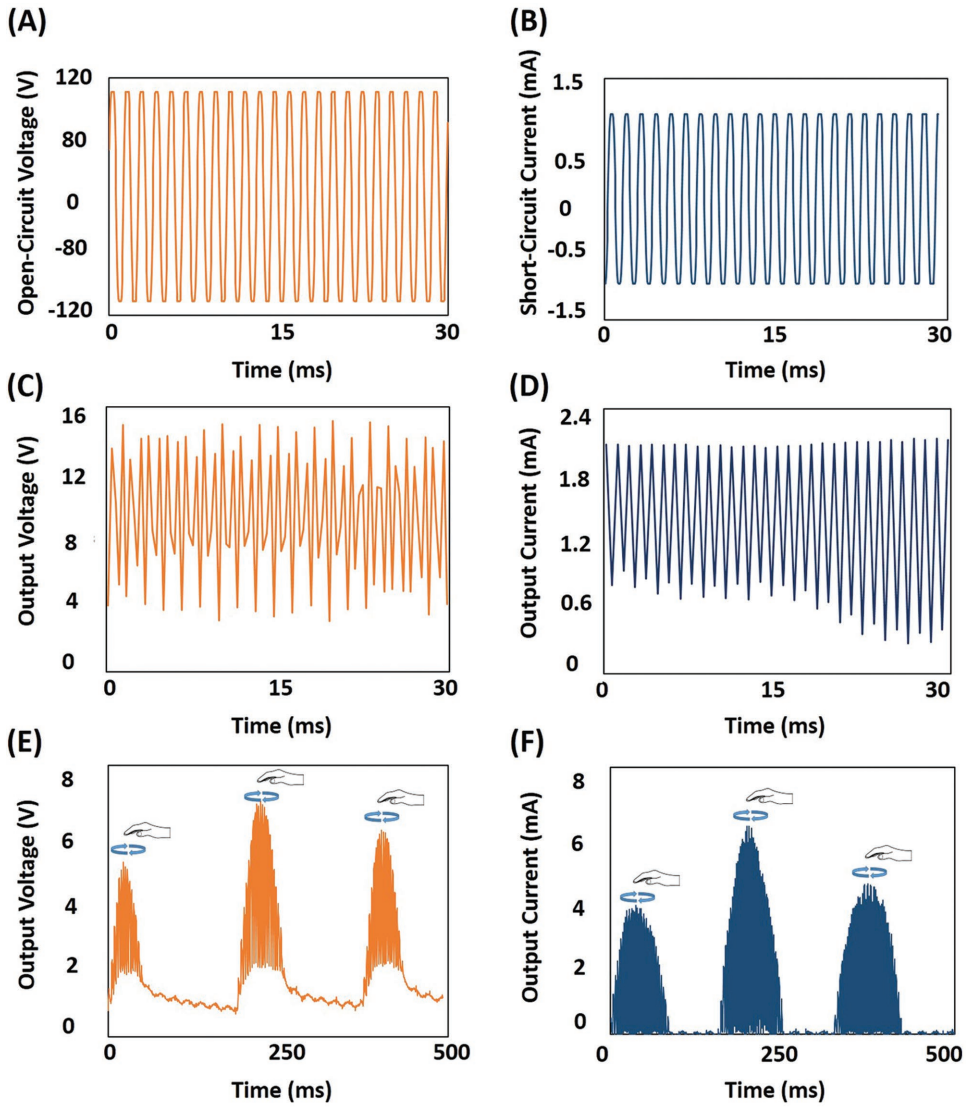

Figure 3. Characterization of the TENG-based self-powered iDDS. A,B) Open-circuit voltage (A) and short-circuit current (B) of TENG under the rotating speed of 500 rpm. C,D) Voltage (C) and current (D) of the TENG applying a transformer and a rectifier. E,F) Voltage (E) and current (F) of TENG under the hand rotating mode (the voltages and currents in the figures were not measured simultaneously).

design can be used to separate drug solution and electrolytes (DI water), reported in our previous publication.[26]

Earlier studies have shown that the electron generation rate in TENG corresponds to the contacting frequency of the Cu metal parts on its two layers.[23] In this experiment, we measured the drug-delivery flow rate by varying the rotation speed of the TENG, as shown in Figure 4G. The measurement is based on quantifying the water flowing distance in the PDMS microtube (Figure 4E,F) and calculated based on Equation (3). When the rotating speed was 300 rpm, the output voltage of the TENG reached about 5 V and the delivery flow rate was about 5.3 μL min^{-1}. We measured a 40 μL min^{-1} flow rate when the rotating speed was 600 rpm. Higher rotating speed may damage the structure of TENG.[27] Considering the primary function of our system is to harvest energy from human's motions that would drive the TENG operating at slow speeds, we have chosen lower rpm values to characterize the performance of TENG-based iDDS. Ways to improve the long-term robustness of TENG have also been reported.[28] The currents applied on the electrochemical pump under different rotating rpms are presented in Figure S5 in the Supporting Information. Previous studies showed that the efficiency of rotating TENG in water electrolysis was calculated to be 43.8%.[23] Generally speaking, higher rotating speeds yield higher delivery flow rates and there is an approximately linear relationship between them. It must be noted that delivery flow rates differ in pumping solutions with different densities. A detailed discussion is provided in the Supporting Information. Indeed, the electrochemical drug pumping was also performed using the energy harvested from the rotation of TENG by human hands (Figure 3E,F). The delivery flow rate in this case was about 1.2 μL min^{-1}. The self-powered drug pumping by hands can be found in Movie S1 in the Supporting Information.

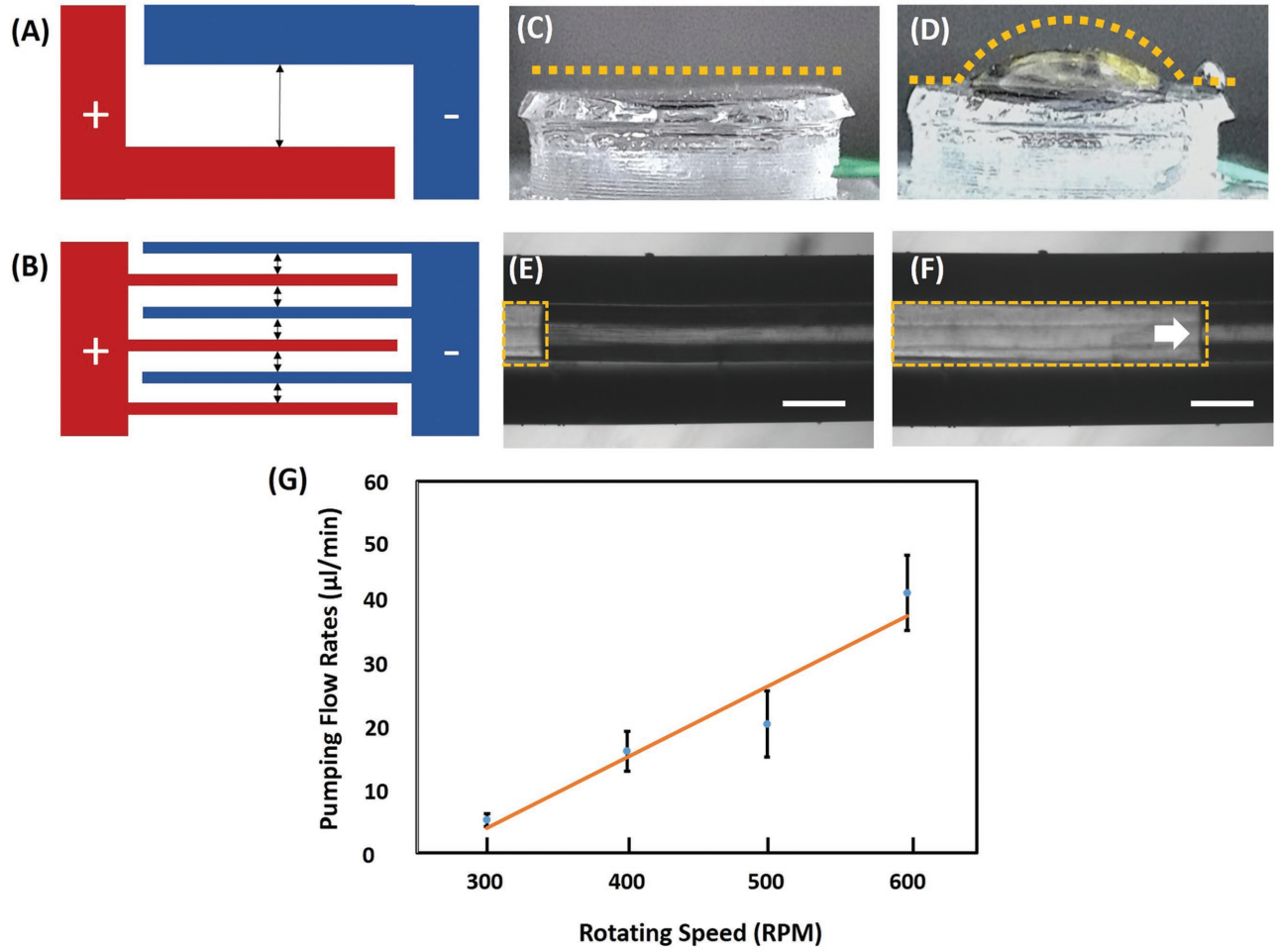

Figure 4. Pumping performance of the TENG-based self-powered iDDS. A,B) Schematic illustration of the conventional electrode and the interdigital electrode design. Black arrow indicates the gap between electrodes. C) Photograph of the drug reservoir before pumping. D) Photograph of the pressurized drug reservoir during pumping. E,F) Microscopy images of water pumped in the PDMS microtube. Scale bars represent 300 µm. G) Pumping flow rate as a function of the rotating speed of TENG. Data are presented as mean ± SD ($N = 5$).

Ex Vivo Trans-Sclera Drug Delivery: As a proof of concept, the self-powered iDDS was tested with enucleated porcine eyes ex vivo. The PDMS microtube was used to penetrate the physiological barrier in ocular drug delivery. A 1 mm incision was made on the sclera and the PDMS microtube of the device was inserted into anterior chamber through the incision (**Figure 5**A,B). This implantation method has been widely used in commercial glaucoma valves (e.g., Ahmed Glaucoma Valve, New World Medical Inc.) and also employed in other ocular drug-delivery studies.[9,29] After implantation, the drug pumping was started by hands operation on TENG to deliver 50 µL volume of micrometer-sized fluorescent particles suspension into the anterior chamber of porcine eyes. The microparticles offer a suitable model to simulate the controlled release of drug carriers and enable fluorescent imaging to trace the delivery.[30] The eye's anterior chamber was then imaged to confirm the success of microparticles delivery (Figure 5D,E). Compared to topical eye drops of large volumes, the trans-sclera drug delivery requires smaller volumes of drug and generates sufficient effects for treating eye diseases such as glaucoma.[31] Clinicians suggest 50–500 nL of daily dosage for sustained treatment, which renders the TENG-based self-powered iDDS with prolonged usability for at least 500 d.[32] This daily dosage is much smaller than the injection volume that could cause rise in intraocular pressure.[33] Moreover, the refillability of the drug reservoir further enhances the working life of the proposed device.

Several iDDSs have been investigated for highly efficient ocular drug delivery.[9,29] However, powering such devices is extremely difficult due to their limited sizes and the clinical restrictions postdevice implantation. In our approach, we offer a TENG-based solution to harvest the endless biokinetic energy for powering the implantable device. This method totally bypasses the needs for external power sources (e.g., battery). Our study shows that the self-powered iDDS could be a viable option to overcome the difficulties in both efficient drug treatment and sustained operation. Having concluded this, we would like to emphasize the developments of TENG that are contributing to advances in designing implantable treatment devices. First, the further miniaturization of TENG has enabled the feasibility of a fully implantable treatment device. The implantable TENG and wearable TENG is able to harvest

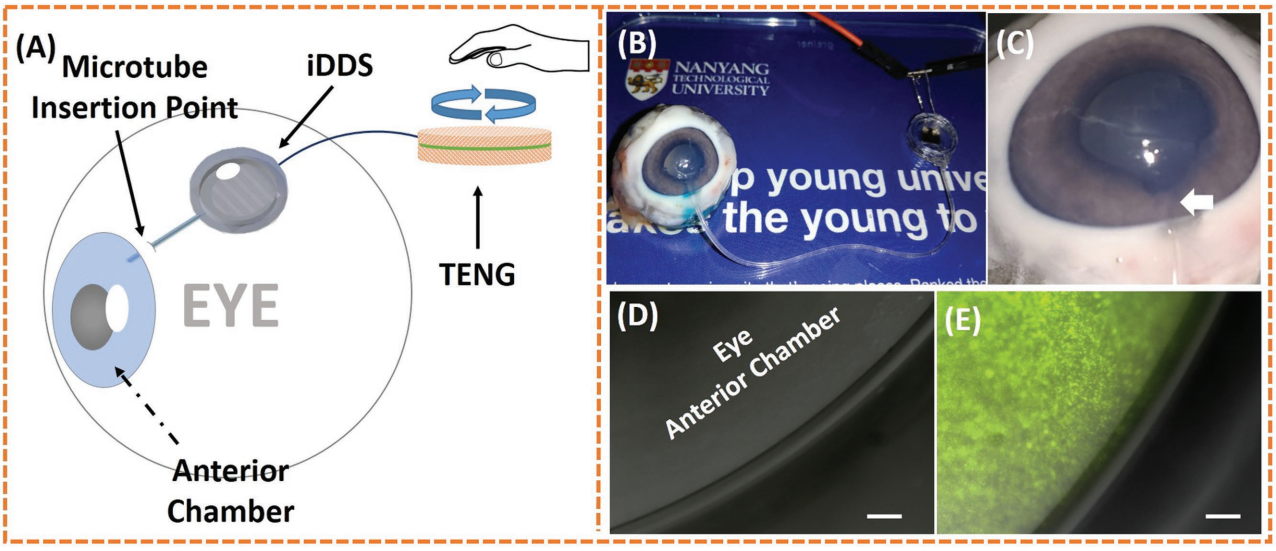

Figure 5. Ex vivo drug delivery study of the TENG-based self-powered iDDS. A) Schematic illustration of the device implantation for drug delivery in the anterior chamber. B) Photograph of the experiment after implantation surgery. C) Amplified photograph of the anterior chamber after PDMS microtube implantation. The white arrow indicates the microtube insertion point. D,E) Fluorescent microscopy of the anterior chamber before and after the delivery of fluorescent microparticles. Scale bars represent 200 µm.

energy directly from organs/tissues' vibrations or slight body motions[2,22] Second, recent reported technology in soft and deformable microneedles device can be combined with the concept of self-powered drug delivery to enable ease-of-use, surgery-free, and battery-less treatment devices.[34] Third, multifunctional micromedical devices have drawn researchers' attention.[35] The noteworthy potential of TENG-based devices in biosensing (e.g., pressure sensing and droplet sensing) has also been investigated.[36] We foresee this unique multifunctional feature of TENG as a major benefit for designing a much smarter iDDS. For example, TENG could be used in monitoring eye pressures in glaucoma treatment and in the meanwhile providing a continuous power for ocular drug delivery for regulating high eye pressure.

In summary, the recent concept of TENG, has been utilized for developing a small size, batteryless implantable treatment device. We present the first TENG-based self-powered iDDS and demonstrate its functionality for ocular drug delivery. Pumping flow rates from 5.3 to 40 µL min^{-1} under different rotating speeds of TENG have been realized. Indeed, the iDDS can be powered with a TENG device rotated by human hand motion. As a proof-of-concept, we demonstrate the ex vivo trans-sclera drug delivery in porcine eyes using the TENG-based self-powered iDDS by utilizing the biokinetic energies of human hands. This work underlines the innovations in TENG-enabled self-powered iDDS for developing novel therapeutic approaches in treating chronic diseases.

Experimental Section

Fabrication of TENG: The TENG was composed of three layers (Figure 1A): i) a layer of metal Cu patterned with radial-arrayed strips, ii) a layer of PTFE film, and iii) another layer of metal Cu patterned with two sets of complementary radial-arrayed electrodes. The metal structure was fabricated by using a standard printed circuit board technology that was reported previously (Figure S1, Supporting Information).[18] The TENG layers were packaged in plastic sheets for motor driving (Figure 1C). Two wires were connected to each side of the electrodes for producing the output current. The PTFE film was flattened and pasted on the layer of Cu electrodes.

Fabrication of iDDS: The iDDS consisted of three parts (Figure 1B): i) an electrochemical pressure pump, ii) a PDMS drug reservoir, and iii) a long microtube. The pressure pump was fabricated by using standard photolithography and e-beam metal-deposition method to achieve the interdigital Au/Ti electrodes on a silicon wafer, as mentioned in our previous publications.[7,26,37] The drug reservoir was fabricated by using PDMS soft lithography method on a 3D printed-ABS mold. The long tube was made by heat curing of PDMS coated on a Tungsten wire. The three parts were assembled together using PDMS as adhesive. The finished device measured 10 mm long, 10 mm wide, and 2 mm high (Figure 1C–E). The tube was 50 mm long, with an outer diameter of 0.6 mm, and inner diameter of 0.3 mm. The electrochemical pressure pump was connected to TENG through the wires. The details of device fabrication can be found in Figure S2 and S3 in the Supporting Information.

Measurement: The TENG was driven by a motor. The output voltage and current of the TENG were measured by low-noise voltage preamplifiers (Keithley 6514 System Electrometer and Stanford Research SR570). The drug-delivery flow rates under TENG rotation at different speeds were measured according to Equation (3). The output current measurement under each rotation speed can be found in the Supporting Information. The volume of water delivered from the device in 60 s was calculated by measuring the liquid moving distance in a PDMS microchannel (Figure 4E,F).

$$\text{Flow Rate}\left(\mu\text{L min}^{-1}\right) = \frac{H(\text{mm}) \times W(\text{mm}) \times D(\text{mm})}{t(\text{min})} \quad (3)$$

In Equation (3), H is the height of the PDMS microchannel, W is the width of the microchannel, D is the flow moving distance measured, and t is the time. The data are presented as the mean volume of water delivered (with standard deviation).

Ex Vivo Ocular Drug-Delivery Study: Enucleated porcine eyes were used to conduct the initial ex vivo studies. The study protocol was approved by the institutional animal care and use committee (IACUC) at Nanyang

Technological University (ARF-SBS/NIE-A0312). A minimally invasive surgical technique was developed to insert the PDMS microtube in the anterior chamber of the eye to achieve trans-sclera drug delivery; drug treatment in this location is needed for treating ocular diseases such as glaucoma. In detail, a 1 mm incision was made on the sclera, then an 18 gauge needle was used to create a tunnel to anterior chamber. A PDMS microtube was inserted into the anterior chamber through the tunnel. Following microtube implantation, the self-powered functionality of the device was tested by operating the human-hand-driven TENG. Fluorescent polystyrene microparticles ($\approx 2 \times 10^7$ particles mL^{-1}, Fluoresbrite YG Microspheres ≈5.7 µm, Polysciences Inc.) in DI water were used to trace the drug perfusion in eye. After delivery, the porcine eyes were imaged under an inverted microscope. The details of the imaging method can be found in Figure S6 in the Supporting Information.

Supporting Information

Supporting Information is available from the Wiley Online Library or from the author.

Acknowledgements

P.S. and S.K. contributed equally to this work. This work was supported from the "thousands talents" program for the pioneer researcher and his innovation team, China, the National Key Research and Development Program of China (Grant Nos. 2016YFA0202704 and 2016YFA0202701), the Singapore Ministry of Education (Grants Tier 2 MOE2010-T2-2-010 (M4020020.040 ARC2/11) and Tier 1 M4010360.040 RG29/10), the NTU–NHG Innovation Collaboration Grant (M4061202.040), the NTU–A*STAR Silicon Technologies, Centre of Excellence, under the program Grant No. 11235100003, the NEWRI seed funding (Grant No. NEWRI SF20140901), and the School of Electrical and Electronic Engineering at NTU. The authors would like to thank Assistant Professor Liu Linbo and Dr. Yu Xiaojun for their assistance with this project.

Received: October 20, 2016
Revised: November 13, 2016
Published online:

[1] C. Chen, Q. Xie, D. Yang, H. Xiao, Y. Fu, Y. Tan, S. Yao, *RSC Adv.* **2013**, *3*, 4473.
[2] Q. Zheng, B. Shi, F. Fan, X. Wang, L. Yan, W. Yuan, S. Wang, H. Liu, Z. Li, Z. L. Wang, *Adv. Mater.* **2014**, *26*, 5851.
[3] V. M. Tronnier, A. Staubert, S. Hähnel, A. Sarem-Aslani, *Neurosurgery* **1999**, *44*, 118.
[4] I. E. Araci, B. Su, S. R. Quake, Y. Mandel, *Nat. Med.* **2014**, *20*, 1074.
[5] P. Cong, N. Chaimanonart, W. H. Ko, D. J. Young, *IEEE J. Solid-State Circuits* **2009**, *44*, 3631.
[6] Y. Sunaga, H. Yamaura, M. Haruta, T. Yamaguchi, M. Motoyama, Y. Ohta, H. Takehara, T. Noda, K. Sasagawa, T. Tokuda, *Jpn. J. Appl. Phys.* **2016**, *55*, 03DF02.
[7] Y. Liu, P. Song, J. Liu, D. Tng, R. Hu, H. Chen, Y. Hu, C. Tan, J. Wang, J. Liu, L. Ye, K.-T. Yong, *Biomed. Microdevices* **2015**, *17*, 1.
[8] E. Meng, R. Sheybani, *Ther. Delivery* **2014**, *5*, 1167.
[9] P. Y. Li, J. Shih, R. Lo, S. Saati, R. Agrawal, M. S. Humayun, Y. C. Tai, E. Meng, *Sens. Actuators, A* **2008**, *143*, 41.
[10] R. Farra, N. F. Sheppard, L. McCabe, R. M. Neer, J. M. Anderson, J. T. Santini, M. J. Cima, R. Langer, *Sci. Transl. Med.* **2012**, *4*, 96.
[11] P. Y. Li, R. Sheybani, C. A. Gutierrez, J. T. W. Kuo, E. Meng, *J. Microelectromech. Syst.* **2010**, *19*, 215.
[12] A. Cobo, R. Sheybani, H. Tu, E. Meng, *Sens. Actuators, A* **2016**, *239*, 18.
[13] L. Halámková, J. Halámek, V. Bocharova, A. Szczupak, L. Alfonta, E. Katz, *J. Am. Chem. Soc.* **2012**, *134*, 5040.
[14] P. P. Mercier, A. C. Lysaght, S. Bandyopadhyay, A. P. Chandrakasan, K. M. Stankovic, *Nat. Biotechnol.* **2012**, *30*, 1240.
[15] S. R. Platt, S. Farritor, K. Garvin, H. Haider, *IEEE/ASME Trans. Mechatron.* **2005**, *10*, 455.
[16] a) A. Zurbuchen, A. Pfenniger, A. Stahel, C. Stoeck, S. Vandenberghe, V. Koch, R. Vogel, *Ann. Biomed. Eng.* **2013**, *41*, 131; b) C. Dagdeviren, B. D. Yang, Y. Su, P. L. Tran, P. Joe, E. Anderson, J. Xia, V. Doraiswamy, B. Dehdashti, X. Feng, *Proc. Natl. Acad. Sci. USA* **2014**, *111*, 1927; c) M. Renaud, P. Fiorini, R. van Schaijk, C. van Hoof, *Smart Mater. Struct.* **2012**, *21*, 049501; d) M. Lee, C. Y. Chen, S. Wang, S. N. Cha, Y. J. Park, J. M. Kim, L. J. Chou, Z. L. Wang, *Adv. Mater.* **2012**, *24*, 1759.
[17] a) S. Wang, Y. Xie, S. Niu, L. Lin, Z. L. Wang, *Adv. Mater.* **2014**, *26*, 2818; b) U. Khan, S.-W. Kim, *ACS Nano* **2016**, *10*, 6429.
[18] C. Han, C. Zhang, W. Tang, X. Li, Z. L. Wang, *Nano Res.* **2015**, *8*, 722.
[19] F.-R. Fan, Z.-Q. Tian, Z. L. Wang, *Nano Energy* **2012**, *1*, 328.
[20] G. Zhu, J. Chen, T. Zhang, Q. Jing, Z. L. Wang, *Nat. Commun.* **2014**, *5*, 3426.
[21] S. Niu, Y. Liu, S. Wang, L. Lin, Y. S. Zhou, Y. Hu, Z. L. Wang, *Adv. Mater.* **2013**, *25*, 6184.
[22] R. Hinchet, S.-W. Kim, *ACS Nano* **2015**, *9*, 7742.
[23] W. Tang, Y. Han, C. B. Han, C. Z. Gao, X. Cao, Z. L. Wang, *Adv. Mater.* **2015**, *27*, 272.
[24] a) C. Hassler, R. P. von Metzen, P. Ruther, T. Stieglitz, *J. Biomed. Mater. Res., Part B* **2010**, *93*, 266; b) S. Kuppusami, R. H. Oskouei, *Univ. J. Biomed. Eng.* **2015**, *3*, 9; c) J.-M. Hsu, L. Rieth, R. A. Normann, P. Tathireddy, F. Solzbacher, *IEEE Trans. Biomed. Eng.* **2009**, *56*, 23.
[25] S. H. Cho, J. Godin, Y. H. Lo, *IEEE Photonics Technol. Lett.* **2009**, *21*, 1057.
[26] P. Song, D. J. H. Tng, R. Hu, G. Lin, E. Meng, K.-T. Yong, *Adv. Healthcare Mater.* **2013**, *2*, 1170.
[27] S. Li, S. Wang, Y. Zi, Z. Wen, L. Lin, G. Zhang, Z. L. Wang, *ACS Nano* **2015**, *9*, 7479.
[28] H. Guo, J. Chen, M.-H. Yeh, X. Fan, Z. Wen, Z. Li, C. Hu, Z. L. Wang, *ACS Nano* **2015**, *9*, 5577.
[29] S. Saati, R. Lo, P. Y. Li, E. Meng, R. Varma, M. S. Humayun, *Curr. Eye Res.* **2010**, *35*, 192.
[30] a) J. A. Cardillo, F. Paganelli, R. A. Costa, A. A. Silva, A. G. Oliveira, A. A. S. Lima-Filho, M. E. Farah, R. B. Jr, B. D. Kuppermann, *Invest. Ophthalmol. Visual Sci.* **2006**, *47*, 3886; b) M. Kumar, J. Pharm, *Pharm. Sci.* **2000**, *3*, 234.
[31] R. Avery, S. Saati, M. Journey, S. Caffey, R. Varma, Y. Tai, M. Humayun, *Invest. Ophthalmol. Visual Sci.* **2010**, *51*, 3799.
[32] R. Lo, P.-Y. Li, S. Saati, R. Agrawal, M. S. Humayun, E. Meng, *Lab Chip* **2008**, *8*, 1027.
[33] A. Smedowski, M. Pietrucha-Dutczak, K. Kaarniranta, J. Lewin-Kowalik, *Sci. Rep.* **2014**, *4*, 5910.
[34] H. Lee, T. K. Choi, Y. B. Lee, H. R. Cho, R. Ghaffari, L. Wang, H. J. Choi, T. D. Chung, N. Lu, T. Hyeon, *Nat. Nanotechnol.* **2016**, *11*, 566.
[35] H. Lee, Y. Lee, C. Song, H. R. Cho, R. Ghaffari, T. K. Choi, K. H. Kim, Y. B. Lee, D. Ling, H. Lee, *Nat. Commun.* **2015**, *6*, 10059.
[36] a) F.-R. Fan, L. Lin, G. Zhu, W. Wu, R. Zhang, Z. L. Wang, *Nano Lett.* **2012**, *12*, 3109; b) L. Lin, Y. Xie, S. Wang, W. Wu, S. Niu, X. Wen, Z. L. Wang, *ACS Nano* **2013**, *7*, 8266; c) S. S. Kwak, S. Lin, J. H. Lee, H. Ryu, T. Y. Kim, H. Zhong, H. Chen, S.-W. Kim, *ACS Nano* **2016**, *10*, 7297.
[37] D. J. Hang Tng, P. Song, R. Hu, C. Yang, K.-T. Yong, *Analyst* **2014**, *139*, 407.